

# PHYSICS MODELS OF EARTHQUAKE

Srutarshi Pradhan\*

*Department of Physics, Norwegian University of Science and Technology, N-7491 Trondheim, Norway*

Since long back, scientists have been putting enormous effort to understand earthquake dynamics -the goal is to develop a successful prediction scheme which can provide reliable alarm that an earthquake is imminent. Model studies sometimes help to understand in some extend the basic dynamics of the real systems and therefore is an important part of earthquake research. In this report, we review several physics models which capture some essential features of earthquake phenomenon and also suggest methods to predict catastrophic events being within the range of model parameters.

## Introduction

'Earthquake' is a long standing problem to the scientist community as it is a subject of many unknowns. Strong earthquakes often causes huge devastation in terms of lives and properties and therefore this subject always demands high priority. But so far, little advancement has been made to understand the entire earthquake-dynamics and the challenge still remains -to develop a successful prediction scheme which can provide exact space-time information of future earthquakes and their expected magnitudes. However, several models and hypothesis [1, 2, 3, 4, 5, 6] have been proposed and some recent studies suggest potential methods to predict catastrophic events in some earthquake models. In this short report we discuss such physics models of earthquake, giving importance to their capability of prediction.

## Geological facts

Plate-tectonic theory explains the origin of earthquake through a stick-slip dynamics: Earth's solid outer crust (about 20 km thick) rests on a tectonic shell which is divided into numbers (about 12) of mobile plates, having relative velocities of the order of few centimeters per year. This motion of the plates arises due to the powerful convective flow of the earth's mantle at the inner core of earth. On the other hand solid-solid frictional force arises at the crust-plate boundary and it sticks them together. This kind of sticking develops elastic strains and the strain energy gradually increases because of the uniform motion of the tectonic plates. Therefore a competition comes to play between the sticking frictional force and the restoring elastic force (stress). When the accumulated stress exceeds the frictional force, a slip (earthquake) occurs and it releases the stored elastic energy in the form of sound, heat and mechanical vibrations. It has been observed that generally a series of small earthquakes appear before (foreshocks) and after (aftershocks) a big quake (main shock).

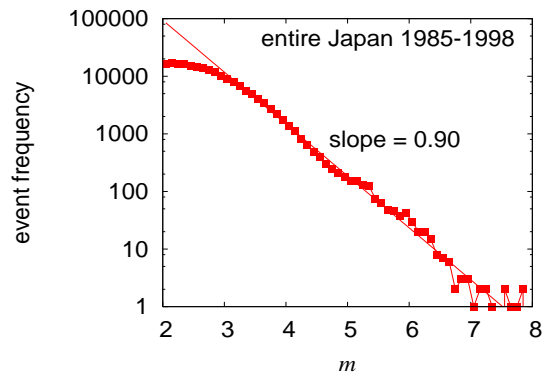


Figure. 1: The magnitude distribution of earthquakes in Japan (from JUNEC catalog) [27]. The straight line with slope  $-0.9$  is the best fit to the data points for  $m > 3$  and supports Gutenberg-Richter law.

## Physics models

The overall frequency distribution of earthquakes including foreshocks, mainshocks and aftershocks, seems to follow the empirical Gutenberg-Richter law [5]:

$$\ln N(m) = \text{constant} - bm,$$

where  $N(m)$  is the number of earthquakes having magnitude (in Richter scale) greater than or equal to  $m$ ,  $b$  is the power exponent. The observed value of  $b$  ranges between 0.7 and 1.0 (Fig.1). The amount of energy  $\epsilon$  released in an earthquake is related to the magnitude as

$$\ln \epsilon = \text{constant} + am.$$

Therefore Gutenberg-Richter law can be expressed as an alternative form:

$$N(\epsilon) = \epsilon^{-\alpha},$$

where  $N(\epsilon)$  is the number of earthquakes releasing energy greater than or equal to  $\epsilon$  and  $\alpha = b/a$ . The Gutenberg-Richter law is being considered as one of the most fundamental observations by the physicists.

Several models have been proposed to study the nature of the earthquake phenomenon. The main intension is to capture the Gutenberg-Richter type power law for the frequency distribution of failures (quakes) by modelling

\*Electronic address: pradhan.srutarshi@ntnu.no

different aspects of faults –structure, material properties, geometry etc. These models can be classified into four groups according to their basic assumptions: (A) Friction models, incorporate the stick-slip dynamics through the collective motion of an assembly of locally connected elements subject to slow driving force (B) Fracture models, look at earthquake phenomena as a fracture-failure process of deformable materials that break under external loading through slow build-up of stress (C) Self-organised critical (SOC) models, consider earthquake as a self-driven slow process and (D) Fractal models, give importance to fractal nature of the crust-plate interfaces and address the phenomenon as a two-fractal overlap problem.

### (A) Friction models

In 1967 Burridge and Knopoff [7] introduced model studies in earthquake research. They proposed a spring-block model to mimic the typical stick-slip dynamics of earthquake phenomena, which has been extended later by Carlson and Langer [8]. The Burridge-Knopoff type model contains a linear array of blocks of mass  $m$  coupled to each other by identical harmonic springs of strength  $k_c$  and also attached to a fixed surface at the top by a different set of identical springs having strength  $k_p$ . The blocks are kept on a horizontal platform (rough surface) which moves with a uniform velocity  $V$  (Fig.2). Here qualitatively the blocks can be thought of as the points of contact between two plates moving at a relative speed  $V$ , where the spring constants  $k_c$  and  $k_p$  represents the linear elastic response of the contact region to compression and shear respectively.

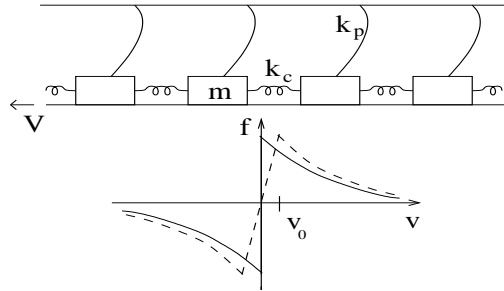


Figure 2: The Burridge-Knopoff model (above) and two different forms of velocity weakening friction force (below) [9].

Starting from unstrained condition, when the system is pulled slowly (at constant rate), the blocks initially remain stuck to the surface due to friction between surfaces. A slip of a block occurs when the corresponding spring force overcomes the threshold value (maximum static frictional force between that block and the rough surface). The dynamics of each block is basically the resultant of two phases: a static phase and a dynamic phase. During static phase the block remains stuck on the rough surface and the elastic strain continuously grows up. The static phase comes to a sudden end when driving force on that block attains the threshold value

and dynamic phase begins. Due to the presence of frictional force this dynamic phase is definitely dissipative in nature. This dissipation reduces the relative velocity of the block and the system again goes back to the static phase. The dynamic friction is assumed as a velocity weakening function  $f$  (shown in the Fig.2). Presence of spring force and velocity weakening friction force leads the system to a complex dynamical state. At the initial stage, individual small slip occurs. But due to constant pulling, the springs are gradually stretched and attain the limit of total frictional stability of the blocks where the collective slips of almost all the blocks occur. Clearly this is a big event and a large amount of elastic energy is released here. The equation of motion of the  $j^{th}$  block of the system is

$$m\ddot{x}_j = k_c(x_{j+1} - 2x_j + x_{j-1}) - k_p x_j - f(\dot{x}_j - V)$$

where dots denote differentiation with respect to  $t$ ,  $m$  is the mass of a block,  $k_p$  and  $k_c$  are spring constants of the connecting springs and  $f$  represents the nonlinear velocity weakening friction force. The position coordinate  $x$  is measured along the chain length and the velocity  $V$  of the platform is in the increasing  $x$  direction. The total energy of the system at time  $t$  can be calculated by solving the above equation. A sudden drops in the energy of the system is identified as the released energy during a slip event and the distribution of such energies follows power-law:

$$N(\epsilon) \sim \epsilon^{-c}, c \sim 1,$$

where  $N(\epsilon)$  is the number of slips releasing energy greater than or equal to  $\epsilon$ .

### Prediction possibility of major events (slips)

Recently Dey et al. [9] developed a method to predict the major slip event in Burridge-Knopoff type spring-block model. Introducing an additional dissipative force in the spring-block arrangement they identified the dissipative functional  $R(t)$  as energy bursts similar to the acoustic emission signals [10, 11] observed in experiments. The distribution of  $R(t)$  shows power laws if one records all slip events including the major slips.

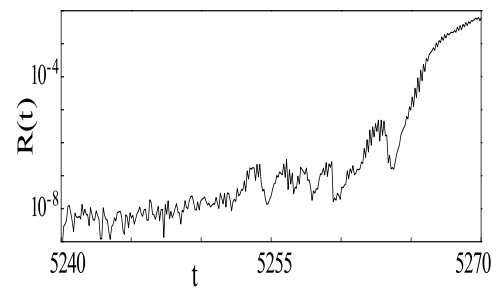


Figure 3: The dissipative functional  $R(t)$  vs. time ( $t$ ) in Burridge-Knopoff model [9].

The plot of  $R(t)$  vs.  $t$  shows a gradual increase in activity (Fig.3) prior to the occurrence of a major slip.

But as  $R(t)$  is noisy it can not help much to predict the major slip event, rather the cumulative energy dissipated  $E_{ae}(t) \sim \int_0^t R(t')dt'$  grows in steps and it seems to diverge as a major slip event is approached (Fig.4). From such divergence one can predict the occurrence time ( $t_c$ ) of a major slip through proper extrapolation.

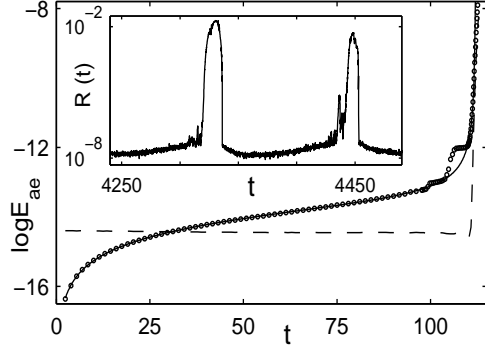


Figure 4: Cumulative energy  $E_{ae}$  versus time ( $t$ ) plot. Inset shows the time series of  $R(t)$  including two major slip events [9].

### (B) Fracture models

Earthquake can be considered as a fracture-failure phenomenon through slow build up of stress at the plate-crust boundary with the movement of the plate as external driving force. The deformation properties of the materials sitting at the boundary play crucial role on spatial redistribution of the stress around a broken region and this actually decides in which direction the crack front should propagate. Fiber bundle model and random fuse model address such scenario in material breakdown and sometimes they are treated as models of earthquake since they produce time series of avalanches which follow power law distribution similar to Gutenberg-Richter law.

#### Fiber bundle model

Fiber bundle (RFB) model consists of many ( $N_0$ ) fibers connected in parallel to each other and clamped at their two ends and having randomly distributed strengths. The model exhibits a typical relaxational dynamics when external load is applied uniformly at the bottom end (Fig.5). In the global load-sharing approximation [12, 13, 14], surviving fibers share equally the external load. Initially, after the load  $F$  is applied on the bundle, fibers having strength less than the applied stress  $\sigma = F/N_0$  fail immediately. After this, the total load on the bundle redistributes globally as the stress is transferred from broken fibers to the remaining unbroken ones. This redistribution causes secondary failures which in general causes further failures and produces an “avalanche” which denotes simultaneous failure of several elements. With steady increase of external load, avalanches of different size appear before the global breakdown where the bundle collapses. The scaling properties of such mean-field

dynamics and the avalanche statistics are expected to be extremely useful in analysing fracture and breakdown in real materials, including earthquakes [15, 16, 17, 18].

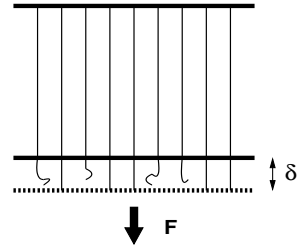


Figure 5: The fiber bundle model .

When external load is applied, the surviving fraction of total fibers follows a simple recursion relation

$$U_{t+1}(\sigma) = 1 - P(\sigma/U_t),$$

where  $U_t = N_t/N_0$ ,  $\sigma$  is the external stress and  $P$  is cumulative probability function. The recursion relation has the form of an iterative map  $U_{t+1} = Y(U_t)$  and finally the dynamics stops at a fixed point where  $U_{t+1} = U_t$ .

If external load is increased in steps by equal amount  $\Delta F$ , then the entire failure process can be formulated through the recursive dynamics [19] mentioned above and the fixed point solution gives the value of critical stress  $\sigma_c$  above which the bundle collapses. It can be shown that the bundle undergoes a phase transition from partially broken state to completely broken state. The order parameter ( $O$ ), susceptibility ( $\chi$ ) and relaxation time ( $\tau$ ) follow robust power laws with universal exponent values [20].

In case of quasi-static load increment, only the weakest fiber (among the intact fibers) fails after loading and then the bundle undergoes load redistribution till a fixed point is reached. The fluctuations in strength distributions produces different size of avalanches during the entire failure process and the avalanche distribution follows power law (Fig.6) with exponent  $-5/2$ . Hemmer and Hansen [14] has analytical proved that this exponent is universal under mild restriction on strength distributions.

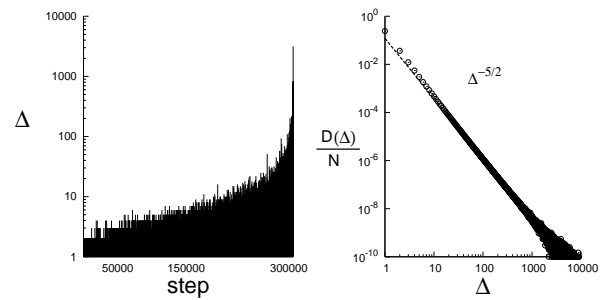


Figure 6: Avalanche time series in a fiber bundle model (left) and the corresponding avalanche distribution (right).

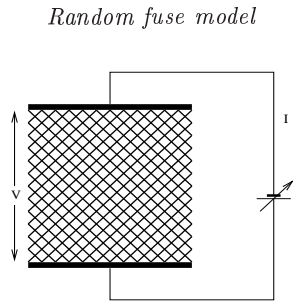


Figure 7: The random fuse model.

The fuse model [21, 22, 23] consists of a lattice in which each bond is a fuse, i.e., an ohmic resistor as long as the electric current it carries is below a threshold value. If the threshold is passed, the fuse burns out irreversibly. The threshold  $t$  of each bond is drawn from an uncorrelated distribution  $p(t)$ . The lattice is placed at  $45^\circ$  with regards to the electrical bus bars (Fig.7) and an increasing current is passed through it. Numerically, the Kirchhoff equations are solved at each node.

When a bond breaks, current value on the neighboring bonds increases and sometimes it triggers secondary failures. Finally the system comes to a state where no current passes through the lattice; that means there is a crack which separates the lattice in two pieces. With gradual increase of current/voltage a series of intermediate avalanches appear before the final breakdown. The distribution of such avalanches follows power law with exponent close to 3 (Fig.8).

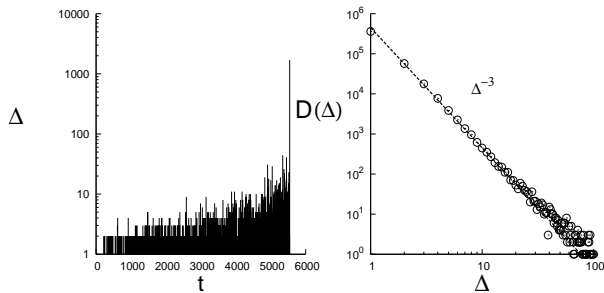


Figure 8: Avalanche time series in a fuse model (left) and the corresponding avalanche distribution (right).

#### Crossover behavior: signature of imminent breakdown

A robust crossover behavior has been observed [24, 25, 26] recently in the two very different models described above where the system gradually approaches the global failure through several intermediate failure events. If intermediate avalanches are recorded, avalanche distribution follows a power law with an exponent that crosses over from one value to a very different value when the system is close to the global failure or breakdown point (Fig.9). Therefore, this crossover is a signature of imminent breakdown.

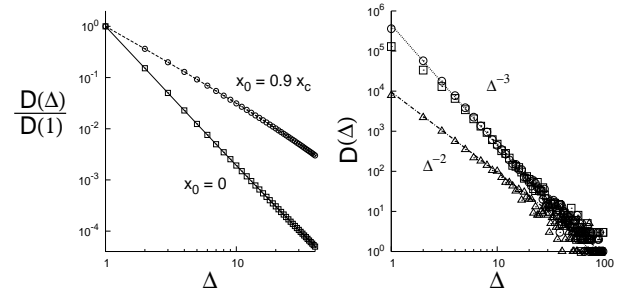


Figure 9: Crossover signature in avalanche power law. In fiber bundle model:  $x_0$  is the starting position of recording avalanches and  $x_c$  is the global failure point; exponent value changes from  $5/2$  to  $3/2$  (left) and in random fuse model: exponent value changes from  $3$  to  $2$  when the system comes closer to breakdown point (right).

Recently Kawamura [27] observed similar crossover behavior for the local magnitude distribution of earthquakes in Japan (Fig.10). This observation has strengthened the possibility of using crossover signal as a tool of predicting catastrophic events.

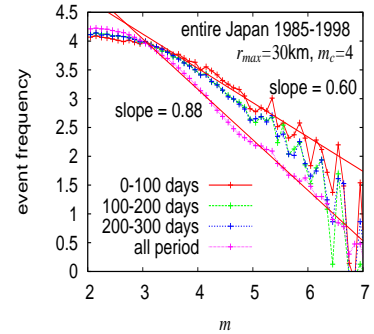


Figure 10: Crossover signature in the magnitude distribution of earthquakes within Japan [27].

#### (C) Self-organised critical models

In various thermodynamics systems, there is a “critical” point where the systems become totally correlated and show scale free (power law) behaviour. Apart from the critical point the average microscopic quantities of the systems follow scaling behaviour. Generally such critical states are achieved through the fine-tuning of physical parameters, such as temperature, pressure etc. and the power law behavior is considered to be a signature of the “critical” state of the system. However, it has been observed that some complex systems evolve collectively to such critical state only through mutual interactions and show power law behavior there. These systems do not need any fine tuning of physical parameter and therefore are considered as “self-organised critical” (SOC) systems. The term SOC was first introduced by Bak, Tang and Wiesenfeld in 1987.

The magnitude distribution of earthquake shows power-law (Gutenberg-Richter law), therefore it is tempting to assume that earthquake happens through a self-organised dynamics: the build up of stress due to tectonic

motion is a self organised slow process; gradually the critical state is achieved where the stress releases in bursts of various sizes. Extensive research have been going on to establish relation between earthquake and SOC systems, for which several models have been proposed. So far, sandpile models are the best example of SOC system.

### BTW sandpile model

The first attempt to study SOC through model systems was made by Bak, Tang and Wiesenfeld [28]. This is a model of sandpile whose natural dynamics drives it towards the critical state. The model can be described on a two dimensional square lattice. At each lattice site  $(i, j)$ , there is an integer variable  $h_{i,j}$  which represents the height of the sand column at that site. A unit of height (one sand grain) is added at a randomly chosen site at each time step and the system evolves in discrete time. The dynamics starts as soon as any site  $(i, j)$  has got a height equal to the threshold value ( $h_{th} = 4$ ): that site topples, i.e.,  $h_{i,j}$  becomes zero there, and the heights of the four neighbouring sites increase by one unit

$$h_{i,j} \rightarrow h_{i,j} - 4, h_{i\pm 1,j} \rightarrow h_{i\pm 1,j} + 1, h_{i,j\pm 1} \rightarrow h_{i,j\pm 1} + 1.$$

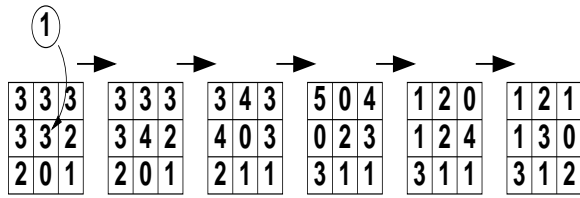


Figure 11: BTW model on square lattice [29].

The process continues till all sites become stable (Fig.11). In case of toppling at the boundary of the lattice (4 nearest neighbours are not available), grains falling outside the lattice are removed and considered to be absorbed/collected at the boundary. Gradually the average height  $h_{av}$  attains a critical value  $h_c$ , beyond which it does not increase at all - on an average the additional sand grains are flown away from the lattice. Total number of toppling between two successive stable states, determines the size of an avalanche and at the critical state avalanche size distribution follows power laws:  $n_s \sim s^{-\Gamma}$ , where  $n_s$  denotes the density of  $s$  size avalanches. The exponent  $\Gamma$  has the value  $\Gamma \simeq 1.15 \pm 0.10$  in 2D [29].

### Manna model

Manna proposed the stochastic sand-pile model [29] by introducing randomness in the dynamics of sand-pile growth. Here, the critical height is 2. Therefore at each toppling, the two rejected grains choose their host among the four available neighbours randomly with equal probability. After constant adding of sand grains, the system

ultimately settles at a critical state having height  $h_c$  and exhibits scale free behavior in terms of avalanche and life time distributions. But the power law exponents are different compared to those in BTW model and therefore Manna model belongs to a different universality class [30].

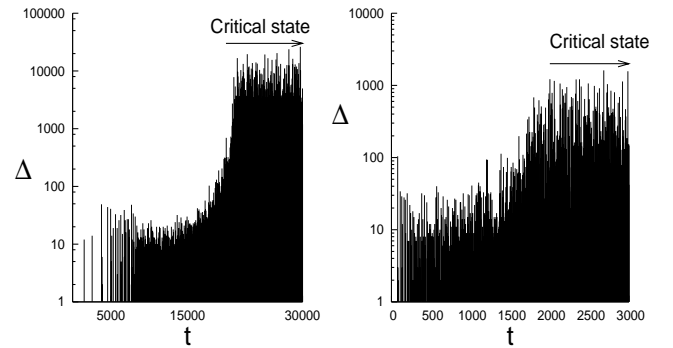


Figure 12: Avalanche time series in a BTW model (left) and in a Manna model (right).

### Precursory activities

On constant adding of grains, sandpile models gradually attains critical state from sub-critical states. Now the question is: can one predict the critical state from the sub-critical response of the pile? A pulse perturbation method [31, 32] gives the answer:

At an average height  $h_{av}$ , a fixed number of height units  $h_p$  (pulse of sand grains) is added at any central point of the system. Just after this addition, the local dynamics starts and it takes a finite time or iterations to return back to the stable state after several toppling events. One can measure the response parameters:  $\Delta \rightarrow$  number of toppling  $\tau \rightarrow$  number of iteration and  $\xi \rightarrow$  correlation length which is the distance of the furthest toppled site from the site where  $h_p$  has been dropped.

To ensure toppling at the target site, the pulse height has been chosen as  $h_p = 4$  for BTW model and  $h_p = 2$  for Manna model. Simulation studies conclude [32] that all the response parameter follow power law as  $h_c$  is approached:  $\Delta \propto (h_c - h_{av})^{-\lambda}$ ,  $\tau \propto (h_c - h_{av})^{-\mu}$ ,  $\xi \propto (h_c - h_{av})^{-\nu}$ ;  $\lambda \simeq 2.0$ ,  $\mu \simeq 1.2$  and  $\nu \simeq 1.0$ . Now if  $\Delta^{-1/\lambda}$ ,  $\tau^{-1/\mu}$  and  $\xi^{-1/\nu}$  are plotted against  $h_{av}$ , all the curve follow straight line and they should touch the x axis at  $h_{av} = h_c$ . A proper extrapolation estimates the critical height  $h_c = 2.13 \pm .01$  for BTW model and  $h_c = 0.72 \pm .01$  for Manna model, which agree well with direct estimates [29].

### Self-affine asperity model

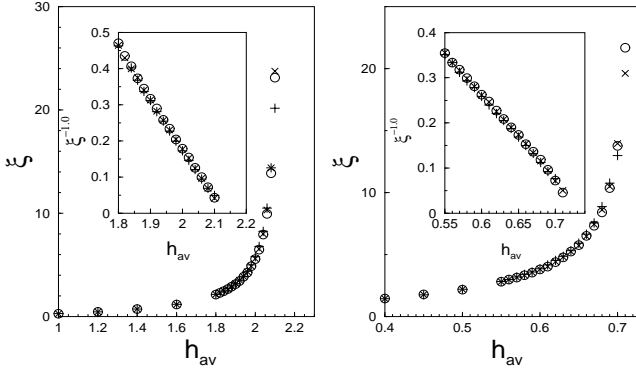


Figure 13: Sub-critical response: Correlation length ( $\xi$ ) versus average height ( $h_{av}$ ) in BTW model (left) and in Manna model (right). Inset shows the plot of inverse  $\xi$  versus  $h_{av}$  and predicts the critical height through extrapolation.

Therefore, although BTW and Manna models belong to different universality classes with respect to their properties at the critical state, both the models show similar sub-critical response or precursors. A proper extrapolation method can estimate the respective critical heights of the models quite accurately.

#### (D) Fractal models

The surfaces of earth's crust and tectonic plate at the fault zone are not compact rather fractal in nature. In fact, these surfaces are the results of the large scale fracture separating the crust from the moving tectonic plate. It has been observed that these surfaces are self similar fractals [33] having the self-affine scaling property  $h(\lambda x, \lambda y) \sim \lambda^\zeta h(x, y)$ , where  $h(x)$  denotes the height of the crack surface at the point  $x$  and  $\zeta$  is the roughness exponent. It has been claimed recently that since the fractured surfaces have got well-characterized self-affine properties, the distribution of the elastic energies released during the slips (earthquake events) between two rough surfaces (crust and plate) may follow the overlap distribution of two fractal surfaces [34, 35]

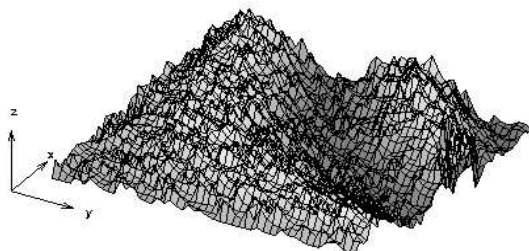


Figure 14: A typical self-affine fracture surface in (2+1) dimension with roughness exponent  $\zeta = 0.8$ .

V. De Rubies et. al. [34] has proposed a new model for earthquakes where the scale invariance of the Gutenberg-Richter law is claimed to come from the fractal geometry of the fault surfaces. In this model the sliding fault surfaces have been represented by fractional Brownian surfaces, whose height scales as  $|h(x+r) - h(x)| \sim r^\zeta$ . The roughness of the surfaces are determined from the value of the exponent  $\zeta$  which lies between 0 and 1. Two surfaces are simulated by two statistically self-affine profiles, say,  $h_1(x)$  and  $h_2(x)$ , one drifting over other with a constant speed  $v$  such that  $h_1(x, t) = h_2(x - vt)$ . An interaction between two profiles represents a single seismic event and the energy released is assumed to be proportional to the breaking area of the asperities. At the contact point of the surfaces the 'surface roughness' prevents slipping and the stress is accumulated there. When the stress exceeds a certain threshold value, breaking (earthquake) occurs. This model produces Gutenberg-Richter type power law:  $P(E) \sim E^{-\beta-1}$ , where  $P(E)dE$  is the probability that an earthquake releases energy between  $E$  and  $E + dE$  and the exponent  $\beta$  is directly related to the roughness exponent  $\zeta$  as :  $\beta = 1 - \zeta/(d-1) = (D_f - 1)/(d-1)$ , where  $D_f$  and  $d$  are respectively the fractal dimension and the embedding dimension of the surfaces.

### Chakrabarti-Stinchcombe model

This is an analytical model, proposed by Chakrabarti and Stinchcombe [35], which incorporates the self-similar nature of both the crust and the tectonic plate. They used self-similar fractals to represent fault surfaces (Fig.15).

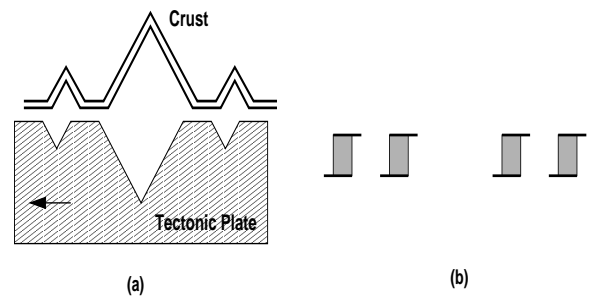


Figure 15: Schematic representation of the rough surfaces of earth's crust and moving tectonic plate [35].

The total contact area between the surfaces is assumed to be proportional to the elastic strain energy that can be grown during the sticking period, as the solid-solid friction force arises from the elastic strain at the contacts between the asperities. This energy is considered to be released as one surface slips over the other and sticks again to the next contact between the rough surfaces. Chakrabarti and Stinchcombe have shown analytically through renormalization group calculations that for

regular fractals (Cantor sets and carpets) the contact area follows power law distribution:

$$\rho(s) \sim s^{-\gamma}; \gamma = 1,$$

which is comparable to that of Gutenberg-Richter law.

### Numerical verification

The claim of Chakrabarti-Stichcombe model has been verified by extensive numerical simulations [36] taking different type of synthetic fractals: regular or non-random Cantor sets, random Cantor sets (in one dimension), regular and random gaskets on square lattice and percolating clusters embedded in two dimensions.

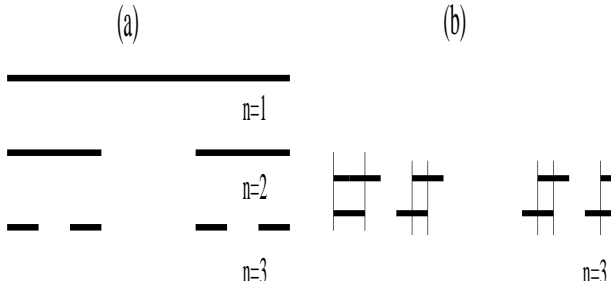


Figure 16: (a) A regular Cantor set of dimension  $\ln 2 / \ln 3$ ; only three finite generations are shown. (b) The overlap of two identical (regular) Cantor sets, at  $n = 3$ , when one slips over other; the overlap sets are indicated within the vertical lines, where periodic boundary condition has been used.

The contact area distributions  $P(m, L)$  seem to follow a universal scaling:

$$P(m, L) \sim L^\alpha P'(m'); m' = mL^\alpha,$$

where  $L$  denotes the size of the fractal and  $\alpha = 2(d - d_f)$ ;  $d_f$  being the mass dimension of the fractal and  $d$  is the embedding dimension. Also the overlap distribution  $P(m)$ , and hence the scaled distribution  $P'(m')$ , decay with  $m$  or  $m'$  following a power law (Fig.17) for both regular and random Cantor sets and gaskets:

$$P(m) = m^{-\beta}; \beta = d.$$

A very recent report [37] analytically explains the origin of such asymptotic power laws in case of Cantor set overlap.

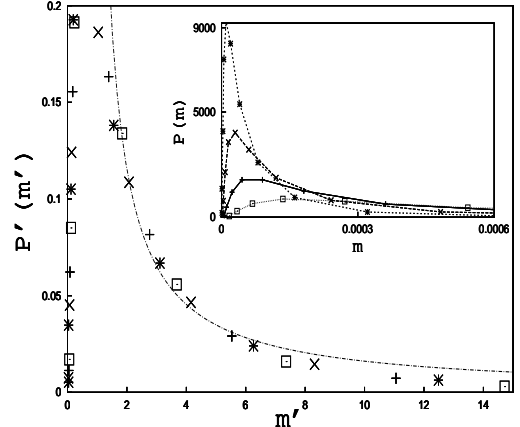


Figure 17: The plot of  $P'(m')$  against  $m'$  for Cantor sets with  $d_f = \ln 2 / \ln 3$  at finite generations:  $n = 10$  (square),  $n = 11$  (plus),  $n = 12$  (cross) and  $n = 13$  (star) and the dotted lines indicate the best fit curves of the form  $a(x - b)^{-d}$ ; where  $d = 1$ . Inset shows  $P(m)$  vs.  $m$  plots.

### Prediction possibility of large events

If one cantor set moves uniformly over other, the overlap between the two fractals change quasi-randomly with time and produces a time series of overlaps  $m(t)$ . Such a time series is shown in Fig.18, for Cantor sets of dimensions  $\ln 2 / \ln 3$ . While most of the overlaps are small in magnitude, some are really big, where as the cumulative overlap size  $Q(t) = \int_0^t mdt$  ‘on average’ grows linearly with time. Is it possible to predict a large future overlap analysing the time series data? A recent study [38] suggests a method:

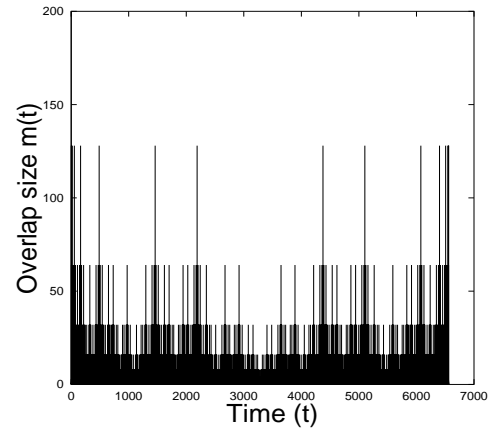
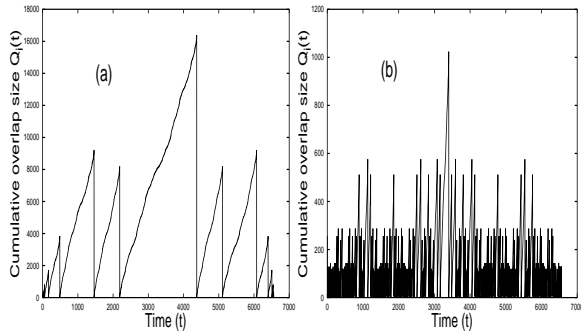


Figure 18: The time ( $t$ ) series data of overlap size ( $m$ ) for regular Cantor sets: of dimension  $\ln 2 / \ln 3$ , at 8th generation.

One can identify the ‘large events’ occurring at time  $t_i$  in the  $m(t)$  series, where  $m(t_i) \geq M$ , a pre-assigned number, then calculate the cumulative overlap size  $Q(t) = \int_{t_i}^{t_{i+1}} mdt$ , where the successive large events occur at times  $t_i$  and  $t_{i+1}$ . Obviously  $Q(t)$  is reset to 0 value after every large event. The behavior of  $Q_i$  with time is

shown in Fig.19 for regular cantor sets . It appears that there are discrete values up to which  $Q_i$  grows with time.



**Figure 19:** The cumulative overlap size variation with time (for regular Cantor sets of dimension  $\ln 2 / \ln 3$ , at 8th generation), where the cumulative overlap has been reset to 0 value after every big event (of overlap size  $\geq M$  where  $M = 128$  and 32 respectively).

Therefore, if one fixes a magnitude  $M$  of the overlap sizes  $m$ , so that overlaps with  $m \geq M$  are called ‘events’ (or earthquake), then the cumulative overlap  $Q_i$  grows linearly with time up to some discrete levels  $Q_i \cong lQ_0$ , where  $Q_0$  is the minimal overlap size, dependent on  $M$  and  $l$  is an integer. This information certainly does not help to predict a future large event accurately, but it gives some hints by identifying discrete levels of  $Q_i$  where a large overlap is likely to happen.

### Discussions and concluding remarks

The Gutenberg-Richter law is a well established law in earthquake research. It should be mentioned that Gutenberg and Richter obtained this law from the statistics of earthquake events observed throughout the world. Also, earthquakes within a tectonically active region (Japan, California etc) follow similar power law. It is still a controversial issue whether the exponent of the Gutenberg-Richter power law is an universal constant or it varies in a narrow range (0.8 to 1.2) depending upon the nature of the fault zone. As the motion of the tectonic plates is surely an observed fact, the stick-slip process should be a major ingredient of earthquake models. Although Burridge-Knopoff type spring-block model successfully captures the stick-slip dynamics and reproduces Gutenberg-Richter type power law in the size distribution of events, it is far from the accurate representation of earthquake dynamics -as it does not contain a mechanism for aftershocks which are observed facts. But this model has some important features: The dynamics is inherently

chaotic -therefore technically unpredictable which agrees well with the occurrence of earthquakes. However, the method proposed by Dey et. al [9] to predict a major slip event by monitoring the cumulative energy function, may open up a wide scope of future research in this field. On the other hand, fiber bundle model and fuse model have been developed basically to study breakdown phenomena in composite materials. As earthquake is a major breakdown phenomenon, these models can be used as earthquake models due to their inherent mean-field nature. Avalanche distributions show power laws in both the models and a crossover in exponent value appears [25] near breakdown point, which can be treated as a criterion for imminent breakdown. SOC models assume a self-driven slow dynamics and reproduces Gutenberg-Richter law at the critical point. Although the critical state can be predicted accurately from the sub-critical response of the systems, the behavior remains unpredictable at the critical state. Fractal overlap models are different (from the other three types) modelling approaches in the sense that they focus on the fractal nature of the fault interfaces and not on the dynamics. The contact area distribution follows asymptotic power law and this suggests a possibility that fractal geometry of the faults might be the true origin of Gutenberg-Richter law.

There are several difficulties in studying earthquake phenomenon, as it is a “N body” complex problem. While exact solution of a 3-body problem needs rigorous mathematical calculations and it does not work for a mutually interacting system having more than 3 bodies, naturally, theoretical physics can not help to formulate the entire earthquake dynamics. Again, as the dynamics of earthquake happens at a depth more than 20 km from earth surface -experimental observation of such dynamics is almost impossible. Moreover, earthquake dynamics involves crust and plates which are highly heterogeneous at many scales from the atomic scale to the scale of tectonic plates, with the presence of dislocation, impurities, grains, water etc and the scenario becomes very much complicated. In this situation, model studies are very important in earthquake research in the sense that they can produce synthetic earthquake events, allow us to monitor the dynamics and analyse the event statistics to compare with the real earthquake data. Moreover, such studies suggest potential methods to predict a major event. It will be a real breakthrough if any of such methods can help a little to predict a future earthquake.

### Acknowledgment:

We are grateful to Bikas. K. Chakrabarti for important collaborations and useful suggestions. Thanks to Research Council of Norway (NFR) for financial support through grant No. 166720/V30.

---

[1] H. J. Herrmann and S. Roux (Eds), *Statistical Models for the Fracture of Disordered Media*, North Holland, Amsterdam (1990).

[2] B. K. Chakrabarti and L. G. Benguigui, *Statistical Physics of Fracture and Breakdown in Disorder Systems*, Oxford Univ. Press, Oxford (1997).

[3] D. Sornette, *Critical Phenomena in Natural Sciences*, Springer-Verlag, Berlin Heidelberg (2000).

[4] M. Sahimi, *Heterogeneous Materials II: Nonlinear and Breakdown Properties*, Springer-Verlag, Berlin (2003).

[5] B. Gutenberg and C. F. Richter, *Seismicity of the Earth and Associated phenomena*, Princeton University Press, Princeton, N.J. (1954).

[6] P. Bhattacharyya and B. K. Chakrabarti (Eds), *Modelling Critical and Catastrophic Phenomena in Geoscience*, Springer, Berlin (2006).

[7] R. Burridge, L. Knopoff, Bull. Seis. Soc. Am. **57** 341 (1967).

[8] J. M. Carlson, J. S. Langer, Phys. Rev. Lett. **62** (1989) 2632-2635.

[9] R. Dey and G. Ananthakrishna, Europhys. Lett. **66**, 715 (2004).

[10] A. Petri, G. Paparo, A. Vespignani, A. Alippi and M. Costantini, Phys. Rev. Lett. **73** 3423 (1994).

[11] A. Garcimartin, A. Guarino, L. Bellon and S. Ciliberto, Phys. Rev. Lett. **79** 3202 (1997).

[12] F. T. Peirce, J. Textile Inst. **17**, T355 (1926).

[13] H. E. Daniels, Proc. R. Soc. London A **183** 405 (1945).

[14] P. C. Hemmer and A. Hansen, ASME J. Appl. Mech. **59**, 909 (1992).

[15] D. Sornette, J. Phys. I (France) **2** 2089 (1992).

[16] D. Sornette, J. Phys. A **22** L243 (1989); A. T. Bernardes and J. G. Moreira, Phys. Rev. B **49** 15035 (1994).

[17] M. Kloster, A. Hansen and P. C. Hemmer, Phys. Rev. E **56** 2615 (1997).

[18] J. V. Andersen, D. Sornette and K. T. Leung, Phys. Rev. Lett. **78** 2140 (1997).

[19] S. Pradhan, P. Bhattacharyya and B. K. Chakrabarti, Phys. Rev. E **66** 016116 (2002).

[20] P. Bhattacharyya, S. Pradhan and B. K. Chakrabarti, Phys. Rev. E **67** 046122 (2003).

[21] A. Hansen and P. C. Hemmer, Phys. Lett. A **184**, 394 (1994).

[22] S. Zapperi, P. Ray, H. E. Stanley and A. Vespignani, Phys. Rev. Lett. **78** 1408 (1997).

[23] S. Zapperi, P. Nukala and S. Simunovic, Phys. Rev. E **71**, 026106 (2005).

[24] S. Pradhan and A. Hansen Phys. Rev. E **72**, 026111 (2005).

[25] S. Pradhan, A. Hansen and P. C. Hemmer Phys. Rev. Lett. **95**, 125501 (2005).

[26] S. Pradhan, A. Hansen and P. C. Hemmer Phys. Rev. E **74**, 016122 (2006).

[27] H. Kawamura, arXiv:cond-mat/0603335 (2006).

[28] P. Bak, C. Tang, K. Weisenfeld, Phys. Rev. Lett. **59** 381 (1987); Phys. Rev. A **38** 364 (1988).

[29] S. S. Manna, J. Stat. Phys. **59**, 509 (1990); P. Grassberger and S. S. Manna, J. Phys. France **51**, 1077(1990); S. S. Manna, J. Phys. A: Math. Gen **24**, L363 (1991).

[30] D. Dhar, Physica A **186**, 82 (1992); Physica A **263**, 4 (1999);Physica A **270**, 69 (1999).

[31] M. Acharyya and B. K. Chakrabarti, Physica A **224**, 254 (1996); Phys. Rev. E **53**, 140 (1996).

[32] S. Pradhan and B. K. Chakrabarti, Phys. Rev. E **65** 016113 (2002).

[33] A. L. Barabasi and H. E. Stanley, (1995). *Fractal Concepts in Surface Growth*, Cambridge University Press, Cambridge.

[34] V. De Rubeis, R. Hallgass, V. Loreto, G. Paladin, L. Pietronero and P. Tosi, Phys. Lett. **76** 2599 (1996).

[35] B. K. Chakrabarti, R. B. Stinchcombe, Physica A, **270** 27 (1999).

[36] S. Pradhan, B. K. Chakrabarti, P. Ray and M. K. Dey, Phys. Scr. T **106** 77 (2003).

[37] P. Bhattacharyya, Physica A **348**, 199 (2005).

[38] S. Pradhan, P. Chaudhuri and B. K. Chakrabarti, in *Continuum Models and Discrete Systems*, Ed. D. Bergman, E. Inan, Nato Sc, Series, Kluwer Academic Publishers (Dordrecht) 245 (2004).